



# CHORUS

This is the accepted manuscript made available via CHORUS. The article has been published as:

## Analysis of Synchronization in a Slowly Changing Environment: How Slow Coupling Becomes Fast Weak Coupling

Jonathan J. Rubin, Jonathan E. Rubin, and G. Bard Ermentrout

Phys. Rev. Lett. **110**, 204101 — Published 13 May 2013

DOI: [10.1103/PhysRevLett.110.204101](https://doi.org/10.1103/PhysRevLett.110.204101)

# Analysis of synchronization in a slowly changing environment: how slow coupling becomes fast weak coupling

Jonathan J. Rubin, Jonathan E. Rubin, and G. Bard Ermentrout  
*Department of Mathematics, University of Pittsburgh*  
 (Dated: April 8, 2013)

Many physical and biological oscillators are coupled indirectly through a slowly evolving dynamic medium. We present a perturbation method that shows that slow dynamics of a coupling medium is effectively equivalent to weak coupling of oscillators. Our methods first apply the theory of averaging to obtain a periodic solution to a single system and then exploit small fluctuations around the mean to analyze coupling between systems. We use this method to explain the spike-to-spike asynchrony seen in a model for bursting neurons coupled through extracellular potassium and to explore synchronization in a model for quorum sensing.

PACS numbers: 05.45.Xt, 87.19.lm, 87.18.Cf

How can fast rhythmic phenomena interact indirectly by influencing a common external medium that may be changing at a rate orders of magnitude slower than their intrinsic time scale? Such issues arise commonly in biological systems with multiple time scales. One relevant example system is a set of neurons firing repeated action potentials or spikes. Each spike that a neuron fires slightly alters ion concentrations in the neighborhood of the neuron. If the neurons lie in sufficiently close spatial proximity that they share extracellular ions, as occurs in many brain regions, then rapid spiking can cause a slow drift in common extracellular ion concentrations, which effectively couples all the neurons [1–3]. A second example arises in synthetic gene networks engineered to provide insights about natural genetic oscillators. In each cell in the relevant networks, gene expression leads to production of corresponding proteins and of an autoinducer. The extracellular autoinducer concentration is sensed by all of the cells, providing an indirect interaction mechanism known as quorum sensing [4, 5]. On quite a different spatial scale, similar issues may arise in ecological settings, where individuals’ short-term behaviors cause gradual changes to a common environment that in turn influences the fast timescale oscillations of population dynamics.

Many decades of computational, theoretical and experimental study have elucidated a wide range of ways that direct coupling can affect oscillator dynamics. A variety of theoretical tools have been developed to facilitate these efforts. In particular, weak coupling theory [6, 7] provides a powerful analytical approach to predict the impact that small direct perturbations have on oscillation phase. Much less is known about effects of indirect coupling through an external medium. Computational studies have revealed possible links between extracellular coupling and brain disorders such as epilepsy and spreading depression (see [8] and references therein). Methods for studying such indirect coupling analytically, however, are in scarce supply.

To impose a common terminology on all such examples, we will refer to an external medium through which oscillators interact as the “bath” and the coupling via

this bath as “bath coupling.” The main result of this paper is a general formula that we derive for the evolution of phases in a network of oscillators interacting through slowly evolving bath coupling, which shows how information about the phase of fast oscillations is transmitted through bath coupling and which can be used to evaluate the stability of phase-locking between pairs of bath coupled oscillators. The derivation harnesses weak coupling theory, even though the size of the bath coupling term in the equation for each oscillator need not be small. We illustrate our results by using them to explain spike desynchronization in a model for epileptogenesis, where spiking neurons interact through a slowly evolving extracellular potassium concentration. Subsequently, we apply our method to study synchrony in a simplified model for quorum sensing.

For our general approach, we consider the following system:

$$\begin{aligned} dX_i/dt &= F(X_i, y), \\ dy/dt &= \epsilon G(X_1, \dots, X_N, y) := \frac{\epsilon}{N} \sum_{j=1}^N g(X_j, y), \end{aligned} \tag{1}$$

where  $X_i$  are vectors of model components that together form the fast subsystem and are modulated by the slowly varying scalar quantity  $y$ , with  $0 < \epsilon \ll 1$  a small parameter. We assume there is a value  $\bar{y}$  such that  $X' = F(X, \bar{y})$  has a  $T$ -periodic stable limit cycle,  $\Phi(t)$ , and that  $\int_0^T g(\Phi(t), \bar{y}) dt = 0$ . These conditions assure that there is a limit cycle solution to  $X' = F(X, y)$ ,  $y' = \epsilon g(X, y)$  for small  $\epsilon$ . Note that in equation (1) there is no interaction between the  $X_i$  if we keep  $y$  constant. While  $y$  is nearly constant, it in fact fluctuates with an  $O(\epsilon)$  magnitude around  $\bar{y}$  and thus communicates weak phasic information among the  $X_i$ . We expand around the limit cycle as  $y = \bar{y} + \epsilon w(t)$  and  $X_i(t) = \Phi(t + \theta_i) + \epsilon \Psi_i(t + \theta_i)$  where  $\theta_i$  are arbitrary phases; we assume that  $\theta_i$  evolve on a slow time scale,  $\tau = \epsilon t$ . The correction terms,  $\Psi_i$ , account for effects in the amplitude and shape of the limit cycle. We see that  $w' = (1/N) \sum_j g(\Phi(t + \theta_j), \bar{y}) + O(\epsilon)$  whence, to leading order,  $w(t) = (1/N) \sum_j p(t + \theta_j)$  where  $p(t) =$

$p(0) + \int_0^t g(\Phi(s), \bar{y}) ds := p(0) + q(t)$ . Note that  $p(0)$  is unknown and that  $p(T) = p(0)$  by our choice of  $\bar{y}$ . The value  $p(0)$  is set by forcing  $(1/T) \int_0^T y(t) dt = \bar{y}$ ; that is, the average of  $p(t)$  must be zero, so  $p(0) = -(1/T) \int_0^T q(t) dt$ .

Now, we return to the coupled system (1), from which we extract the  $O(\epsilon)$  equation

$$\begin{aligned} \Psi'_i(t + \theta_i) &= F_x(\Phi(t + \theta_i), \bar{y}) \Psi_i(t + \theta_i) - \Phi'(t + \theta_j) \frac{d\theta_i}{d\tau} \\ &+ F_y(\Phi(t + \theta_i), \bar{y}) \frac{1}{N} \sum_{j=1}^N p(t + \theta_j). \end{aligned}$$

This is a classic weak coupling equation (see for example [9]) and we can immediately characterize the evolution of the phases:

$$d\theta_i/d\tau = \frac{1}{N} \sum_{j=1}^N H(\theta_j - \theta_i), \quad (2)$$

$$H(\phi) = \frac{1}{T} \int_0^T Z(t) \cdot F_y(\Phi(t), \bar{y}) p(t + \phi) dt. \quad (3)$$

Here,  $Z(t)$  satisfies the adjoint equation  $Z'(t) = -[F_x(\Phi(t), \bar{y})]^T Z(t)$  with  $Z(t) \cdot \Phi'(t) = 1$ . For  $N = 2$ , we can write a single equation for  $\phi = \theta_2 - \theta_1$ , which takes the form

$$d\phi/d\tau = H(-\phi) - H(\phi) = -2H_{odd}(\phi). \quad (4)$$

Zeros of  $H_{odd}(\phi)$  are phase-locked states; those for which  $H'_{odd}(\phi) > 0$  are asymptotically stable while  $H'_{odd}(\phi) < 0$  implies instability. We next illustrate our results in two specific models.

Simulations of bath coupled neuron pairs, described by a model linking the dynamics of membrane potential and of ion concentrations, exhibit synchronized bursting activity, with alternating quiescent and spiking periods [8]. Within each burst, however, the neurons' spikes occur out-of-phase. It has been shown previously that the out-of-phase firing of spikes within bursts has the potential to extend the parameter range over which bursting occurs, to prolong active phases of bursts, and to alter burst frequency [10–13]. We thus consider spike synchrony in a bath coupled model [8]. This model comprises Hodgkin-Huxley type equations for the membrane voltages,  $V_j(t)$ , of two cells, along with equations for the cells' intracellular sodium concentrations and the shared extracellular potassium concentration:

$$CdV_j/dt = -(I_{Na}(V_j, h_j) + I_K(V_j, n_j) + I_L(V_j)) \quad (5)$$

where  $I_{Na}(V, h) = g_{Na} m_\infty(V) h(V - E_{Na})$ ,  $I_K(V, n) = g_K n^4 (V - E_K)$ , and  $I_L(V) = g_{Na,L}(V - E_{Na}) + g_{K,L}(V - E_K) + g_{Cl,L}(V - E_{Cl})$  are transmembrane sodium, potassium, and leak currents, respectively. In these expressions,  $m_\infty(V_j)$ ,  $n_j$ , and  $h_j$  are gating variables, with  $n_j, h_j$  governed by equations of the form  $dx/dt = \phi(\alpha_x(V))(1 - x) - \beta_x(V)x$ . Critically for our study,

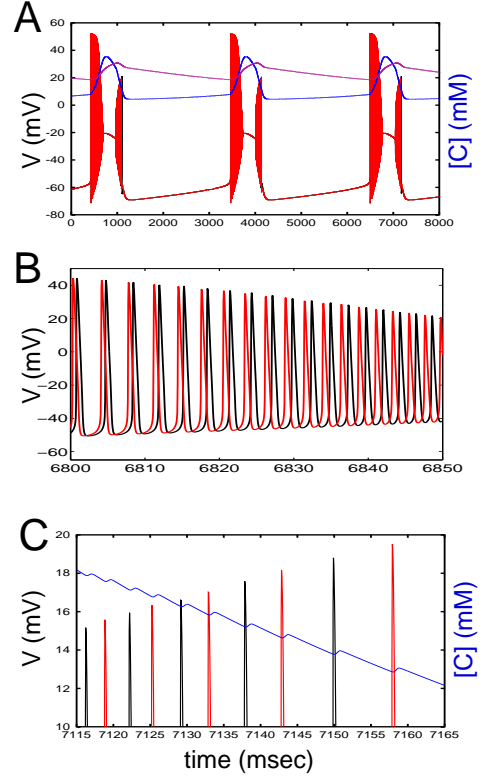


FIG. 1: Synchronized bursting in the two-cell model. (A) One cell's membrane potential (red), the shared extracellular potassium concentration (blue), and one cell's intracellular sodium concentration (magenta). The two cells' potentials and sodium concentrations are indistinguishable on this scale due to a high level of synchrony. (B) Magnified view of both cells' potentials near the onset of spiking within a burst reveals the development of asynchronous spiking. (C) A zoomed view of a burst showing small fluctuations in the potassium concentration during spiking.

sodium and potassium reversal potentials in mV are not constant but are specified by the Nernst equations  $E_{Na} = 26.64 \ln([Na]_o/[Na]_i)$  and  $E_K = 26.64 \ln([K]_o/[K]_i)$ . The intracellular ( $i$ ) and extracellular ( $o$ ) ion concentrations, in mM, obey the equations ( $j = 1, 2$ ):

$$\begin{aligned} d[K]_o/dt &= \epsilon(\gamma\beta/2)(I_K(V_1, n_1) + I_K(V_2, n_2)) \quad (6) \\ &- \beta[\tilde{I}_{pump}([Na]_i)_1 + \tilde{I}_{pump}([Na]_i)_2] \\ &- \tilde{I}_{glia}([K]_o) - \tilde{I}_{diff}([K]_o) \end{aligned}$$

$$d([Na]_i)_j/dt = \epsilon \left( -\gamma I_{Na}(V_j, h_j) - 3\tilde{I}_{pump}([Na]_i)_j \right),$$

$([K]_i)_j = 158 - ([Na]_i)_j$ , and  $[Na]_o = 144 - (\beta/2)[([Na]_i)_1 + ([Na]_i)_2 - 36]$ . The latter two relations are based on conservation of sodium and the relation of sodium and potassium transport [14, 15], while  $\gamma, \beta, \rho$  are parameters used to convert units and account for differences in intracellular and extracellular volumes. The equation for  $[K]_o$  is modified from the original [8] to take into account that both neurons share a common extracellular potassium supply; we also changed

$\epsilon$  from  $10^{-3}$  to  $10^{-2}$  to speed up simulations while leaving model dynamics qualitatively unchanged in the regime we considered. The components of equation (6) are the outward potassium current  $I_K$  from equation (5), a potassium/sodium pump current  $\tilde{I}_{pump}([Na]_i) = \rho[1 + \exp((25 - (Na)_i)/3)]^{-1}[1 + \exp(5.5 - [K]_o)]^{-1}$ , a glial potassium uptake current  $\tilde{I}_{glia} = G[1 + \exp((18 - [K]_o)/2.5)]$ , a diffusion current  $\tilde{I}_{diff} = \eta([K]_o - k_{bath})$ , and the inward sodium current  $I_{Na}$  from equation (5), with the parameters  $G = 20mM/s, \eta = 0.133Hz$  and  $k_{bath} = 22mM$  selected to focus on a particular type of bursting solution (see Figs. 3B-4B of [8]).

For a model network of two cells, parameters could be tuned to give similar types of bursting behavior to those reported previously for a single cell [8]. Within the bursting solutions that we consider, the timing of the active phase periods for the two cells was tightly synchronized (Fig. 1A). While voltages were synchronized during quiescent phases of each burst, some voltage desynchronization occurred as soon as cells started to spike, with a progressive shift towards anti-phase spiking over the course of active phase (Fig. 1B). Interestingly, the particular bursts shown in Fig. 1 included periods where spiking was interrupted by depolarization block; although voltages appeared to be synchronized during each depolarization period, some phase information appeared to be maintained, such that the cells' spikes were phase-shifted when they resumed.

Fig. 1C offers a more magnified view of the time course of  $[K]_o$  and shows small fluctuations around a slow drift during the active phase of each burst. Since the coupling between cells in the model occurs only through  $[K]_o$ , these  $[K]_o$  fluctuations provide a means to communicate spike-by-spike phase information. To understand how this communication occurs we now apply the above theory.

For model (5)-(6), we would like to equate each fast spiking event within a burst to the limit cycle  $\Phi$  in the general theory, with slow variable  $[K]_o$ . In fact, the individual spikes do not correspond to a true limit cycle of the fast subsystem; over each spike,  $[K]_o$  does not fluctuate around a constant value but rather around a slowly drifting baseline. But, the phase information in each spike is independent of this drift. Thus, to evaluate the stability of phase-locking at a particular point on the orbit of a burst, we choose the  $[K]_o$  there and use this as our  $\bar{y}$ , and we add a constant to the right hand side of the  $[K]_o$  equation in (6) to remove the slow drift. Generally, for model (1), we can adjust the  $y$  equation to  $y' = \epsilon[G(X_1, \dots, X_N, y) + k]$  for  $k = -(1/T) \int_0^T g(\Phi(t), \bar{y}) dt$  to attain the mean value  $\bar{y}$  and eliminate any baseline drift, such that the above theory applies. Since the other slow variables  $[Na]_i$  are intracellular and thus communicate no phasic information, we simply fix them at the values they take at the selected point on the orbit.

In sum, we select a point within the burst and compute the corresponding fast subsystem periodic orbit, the

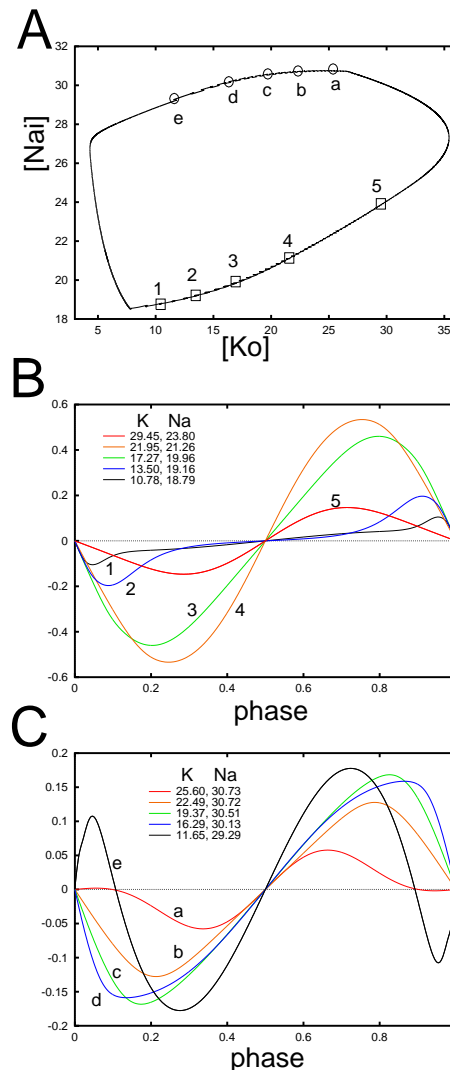


FIG. 2: Analysis of spike desynchronization for model (5)-(6). (A) Phase plane projection of  $[K]_o$  and  $[Na]_i$  for one cell during a burst. Sample points used for averaging are labeled. (B) Odd part of the interaction function,  $H_{odd}(\phi)$ , for the five squares in panel (A) showing that synchrony is unstable and anti-phase spiking is stable. Phase has been rescaled to lie between 0 and 1. (C)  $H_{odd}(\phi)$  for the five circles in panel (A). Anti-phase is always stable while synchrony is unstable except at low and high  $[K]_o$ .

constant  $k$ , the resulting  $w(t)$  from the adjusted  $y$  equation, and the voltage component of the adjoint solution,  $V^*(t)$ . From these, we compose the interaction function, which for this model is  $H(\phi) = (1/T) \int_0^T 26.64V^*(t)w(t + \phi)[g_K n^4(t) + g_{K,l}]/(C\bar{K}) dt$ , where  $\bar{K}$  is the value of  $[K]_o$  at the selected point. Fig. 2B shows  $H_{odd}(\phi)$  for the points labelled by the five squares on the lower part of the  $[K]_o - [Na]_i$  projection of a burst, shown in Fig. 2A. (We note that the lower segment corresponds to the first part of the burst in Fig. 1A and the upper segment to the second smaller part of the burst.) In all cases the slope through the rescaled phase,  $\phi = 1/2$ , is positive, which

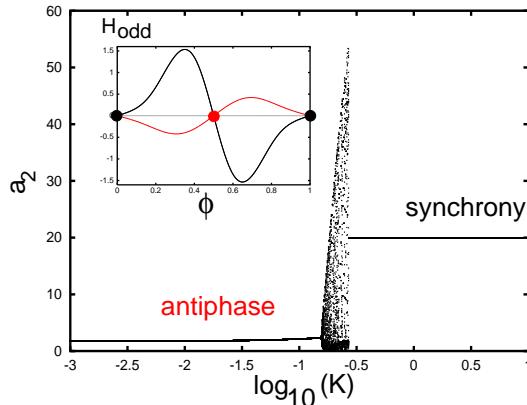


FIG. 3: Stability diagram for a pair of bath-coupled repressors governed by (7). Parameters are  $\kappa = 0.2$ ,  $\alpha = 216$ ,  $\beta = 1$ ,  $\eta = 1$  with  $K$  varying between slow and fast. For  $K$  large enough, synchrony is the only attractor while for  $K$  small, the anti-phase solution is stable. Inset:  $H_{odd}(\phi)$  for the two limits,  $K \rightarrow \infty$  (fast, black) and  $K \rightarrow 0$  (slow, red). In these extremes anti-phase and synchrony exchange stability.

means that the anti-phase solution is stable. Additionally, the slope through 0 is always negative so that synchrony is unstable. Thus, over the entire transit through the first part of the burst, spikes will be pushed into anti-phase. Fig. 2C shows  $H_{odd}(\phi)$  for the second part of the burst at the points labelled by circles in the top segment of the orbit in Fig. 2A. At the start of this part of the burst, synchrony is very weakly stable ( $H'_{odd}(0) > 0$  for  $[K]_o = 25.60$ ) and anti-phase is also stable. However, by the time  $[K]_o$  has dropped to 22.49, synchrony loses stability and the only stable state is anti-phase, such that spiking becomes progressively closer to anti-phase as the burst evolves. Near the end of the burst, synchrony becomes stable again, but since anti-phase is still stable, anti-phase spiking continues through the termination of the oscillatory activity. This analysis provides an intuitive mechanism for the active desynchronization of spikes during a slow passage through a burst: small fluctuations of the bath coupling around a slowly drifting mean provide information about spike timing that acts as a weak coupling to push spike times apart.

There has been a great deal of interest in the coupling of genetic and other regulatory systems in bacteria and other organisms. In [4], the authors showed that bacteria transfected with a set of genes that generate an autonomous oscillation (the repressilator) were able to synchronize through quorum sensing, namely coupling via an autoinducer dependent on proteins produced by all population members. A weak coupling analysis was performed under the assumption that the coupling through this shared bath was instantaneous. Here, we allow the bath  $M$  to evolve over a range of time scales and apply weak coupling analysis and our new slow coupling analysis to show that there is a switch from synchrony to

anti-phase activity for a coupled pair of cells. The model equations ( $i = 1, 2$ ) are

$$\begin{aligned} da_i/dt &= -a_i + \alpha/(1 + C_i^2), & dA_i/dt &= \beta(a_i - A_i), \\ db_i/dt &= -b_i + \alpha/(1 + A_i^2), & dB_i/dt &= \beta(b_i - B_i), \\ dc_i/dt &= -c_i + \alpha/(1 + B_i^2) + \kappa(M - c_i), \\ dC_i/dt &= \beta(c_i - C_i), \\ dM/dt &= K[-M + \eta(\frac{c_1 + c_2}{2} - M)]. \end{aligned} \quad (7)$$

As in [4], we couple to the bath via the variable  $c$ . We use a simpler form of coupling (linear diffusive) than was used in [4] as it allows us to compare the slow and fast coupling more directly.

In [4], the analysis was done in the limit as  $K \rightarrow \infty$  (the quasi-steady state hypothesis) and it was assumed that  $\kappa$  was small, so that a weak coupling analysis would apply. Fig. 3 shows a “stability” diagram for (7) as  $K$  varies between  $10^{-3}$  and 10. The value of  $a_2(t)$  is plotted each time  $a_1(t)$  increases through 20. For each  $K$ , we start near the synchronous solution and let the system evolve for 10000 time units (the period is about 15 time units) and plot only the points from the last 1000. For  $K$  larger than  $10^{-0.4}$ , synchrony is stable and for  $K$  smaller than about  $10^{-0.7}$ , anti-phase is stable. In between, a complex series of bifurcations occurs. To understand the result for large  $K$  (“fast”), we set  $M$  to its quasi-steady state value so that the coupling becomes  $\kappa[(c_1 + c_2)\eta/[2(1 + \eta)] - c_i]$  and an application of weak coupling theory leads to  $H_{fast}(\phi) = \frac{\kappa}{2T(1+\eta)} \int_0^T c^*(t)[c(t + \phi) - (\eta + 1)c(t)] dt$ . Here  $c^*(t)$  is the  $c$ -component of the adjoint and  $c(t)$  is the  $c$ -component of the isolated limit cycle. In the odd part of  $H_{fast}$ , the slope through 0 is positive (Fig. 3, inset) and the slope through 0.5 is negative, so synchrony is stable and anti-phase unstable. We next apply the theory developed in this paper to handle the case when  $K \rightarrow 0$ . (We remark that for this case,  $\kappa$  need not be small; we chose a small value of  $\kappa$  so we could compare to the fast coupling case.) In this case,  $H_{slow}(\phi) = \frac{\kappa}{2T} \int_0^T c^*(t)[p(t) + p(t + \phi)] dt$  where  $p(t) = p(0) + \int_0^t c(s) ds$ . The slope of the odd part of  $H_{slow}$  at 0.5 is positive and at 0 is negative (Fig. 3, inset), so synchrony is unstable and anti-phase stable. Interestingly, the interaction for fast bath coupling depends on  $c(t)$  while for slow coupling it depends on the integral of  $c(t)$ .

Weak coupling theory, based on averaging over the period of an underlying limit cycle oscillation, provides an effective way to assess the stability of phase relations resulting from small magnitude interactions transmitted instantaneously between coupled oscillators [6, 7]. In this paper, we have considered systems with large magnitude interactions, which would appear to be outside the scope of weak coupling theory. Two insights, however, allow us to extend the mathematics of weak coupling theory to this scenario. First, in a limit in which coupling becomes constant in time, the oscillators become uncoupled, so small fluctuations about a large constant coupling term

act like weak coupling. Second, small fluctuations around a slowly drifting coupling term act like small fluctuations around a constant coupling term. Using these insights, we show that for two neurons coupled through a shared extracellular potassium concentration, in a certain bursting regime, the neurons' bursts synchronize but the spikes they fire within these bursts are pushed away from synchrony by the phase information within each spike. While the physical reasoning for why  $H'(0) < 0$  is outside the scope of our mathematical theory, increased extracellular potassium due to release during a slightly leading spike could either prolong or truncate a following spike, and our theory suggests that the former effect is dominant. Our

theory also goes beyond previous results to demonstrate that quorum sensing in genetic oscillators may or may not yield synchronization depending on the time scale at which the coupling medium evolves, with destabilization of synchrony for a sufficiently slow medium.

### Acknowledgments

This work was partially supported by NSF Awards EMSW21-RTG0739261, DMS1021701, and DMS1219753.

- 
- [1] G. G. Somjen, *Ions in the Brain* (Oxford University Press, New York, 2004).
- [2] F. Fröhlich, M. Bazhenov, V. Iragui-Madoz, and T. Sejnowski, *The Neuroscientist* **14**, 422 (2008).
- [3] D. Durand, E.-H. Park, and A. Jensen, *Phil. Trans. Roy. Soc. B: Biolog. Sci.* **365**, 2347 (2010).
- [4] J. Garcia-Ojalvo, M. Elowitz, and S. Strogatz, *Proc. Nat. Acad. Sci. USA* **101**, 10955 (2004).
- [5] T. Danino, O. Mondragón-Palomino, L. Tsimring, and J. Hasty, *Nature* **463**, 326 (2010).
- [6] G. Ermentrout and D. Terman, *Mathematical Foundations of Neuroscience* (Springer, New York, 2010).
- [7] M. Schwemmer and T. Lewis, in *Phase Response Curves in Neuroscience: Theory, Experiment, and Analysis* (Springer, 2012).
- [8] E. Barreto and J. Cressman, *J. Biol. Phys.* **37**, 361 (2011).
- [9] Y. Kuramoto, *Chemical Oscillations, Waves, and Turbulence* (Dover Publications, 2003).
- [10] A. Sherman and J. Rinzel, *Proc. Nat. Acad. Sci. USA* **89**, 2471 (1992).
- [11] A. Sherman, *Bull. Math. Biol.* **56**, 811 (1994).
- [12] G. de Vries and A. Sherman, in *Bursting: The Genesis of Rhythm in the Nervous System* (World Scientific, Singapore, 2004), pp. 243–272.
- [13] J. Best, A. Borisyuk, J. Rubin, D. Terman, and M. Wechselberger, *SIAM J. Appl. Dyn. Syst.* **4**, 1107 (2005).
- [14] J. Cressman, G. Ullah, S. Schiff, and E. Barreto, *J. Comput. Neurosci.* **26**, 159 (2009).
- [15] J. R. Cressman, G. Ullah, J. Ziburkus, S. J. Schiff, and E. Barreto, *J. Comput. Neurosci.* **30**, 781 (2011).